A. Murrone, P. Villedieu

(Onera)

E-mail: angelo.murrone@onera.fr

Numerical Modeling of Dispersed Two-Phase Flows

This paper presents some fundamental aspects of the mathematical and numerical modeling of dispersed two phase flows. The special case of gas-particle flows which is of major importance in the aerospace context is examined. The "kinetic" equation corresponding to the mesoscopic level of description is recalled and the derivation of the different models is explained. Microscale physical phenomena occurring in gas-particle flows are also described. Then an overview of the different numerical methods is given. The SPARTE and SPIREE solvers of the CEDRE code illustrate Lagrangian and Eulerian techniques respectively, implemented in a 3D complex CFD platform. Some numerical simulations are presented, showing the capacity of the solvers to deal with turbojet engines, liquid rocket engines, solid propellant rockets, icing problems, etc. The advantages and drawbacks of Lagrangian and Eulerian techniques are briefly discussed, from the theoretical and practical points of view. We also present the future developments expected in the code, taking into account the crucial challenges in numerical simulation such as Large Eddy Simulation, primary atomization, coupling "separated" and "dispersed" two-phase flow solvers, spray-film interactions.

Introduction

The topic of two-phase flows has, in a wide variety of engineering systems, become increasingly important for optimal design and safe operations. A non-exhaustive list of examples including power systems, heat transfer systems, chemical engineering and transport systems shows that a classification is needed in order to derive the various models.

Classification of two-phase flows

For modeling purposes we need to introduce a classification for the large variety of two-phase flows. This classification depends mainly on both the physical state of the two phases and on the flow structure. First, as regards the physical state, four combinations can be considered: gas-solid, gas-liquid, liquid-solid and liquid-liquid mixtures. Then, for the structure, and especially the interface topology, it is more difficult to establish a set of combinations because changes in the flow may be occurring continually. Nevertheless, following the work of Ishii [18], two-phase flows are generally classified into three categories according to the shape of the interface: separated flows, mixed flows and dispersed flows, as explained in Box 1.

In this paper, we shall focus on the class of dispersed two-phase flows (and more precisely on the special case of gas – particle flows) which is of major importance for many applications in the aerospace context. A set of examples is given in the next section.

Dispersed two-phase flows in aerospace systems

Dispersed two-phase flows are involved in most aerospace propulsion systems. In turbojet engines, for example, kerosene is stored in a condensed form and injected as a spray of small droplets in the combustion chamber. Flame ignition and stability depend to a large extent on the droplet dynamics and evaporation (Figure 1 page 3). For modeling purposes, two different zones may be considered: the primary break-up zone located in the vicinity of the nozzle exit where the liquid jet is atomized into small droplets, and the spray zone where droplets are already formed and are carried by the gas flow. In the first zone, the liquid phase is continuous and a separated two-phase flow model needs to be used while in the spray zone a dispersed flow description is more appropriate.

Box 1 - Classification of Two-phase flows

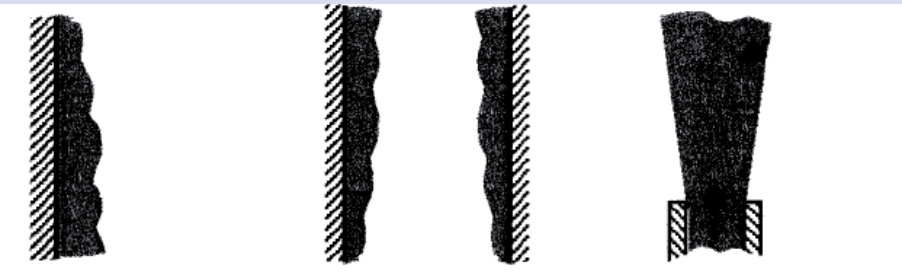

Figure B1 - 01 - Separated two-phase flows: film flow, annular flow and jet flow

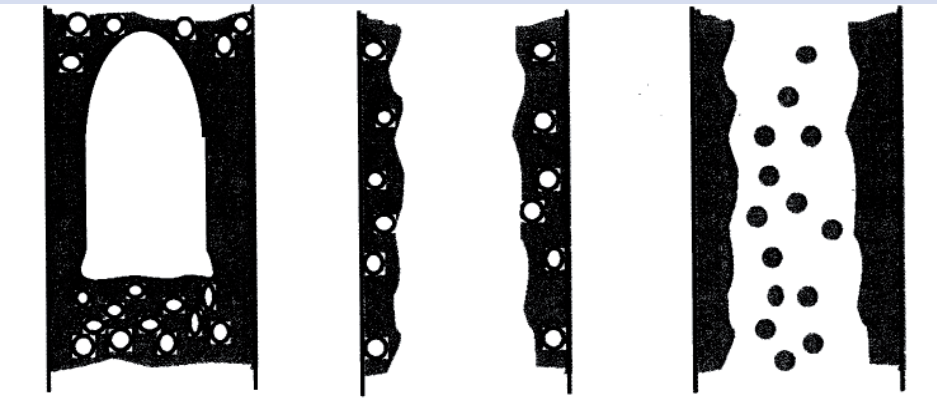

Figure B1 - 02 - Mixed two-phase flows: slog or plug flow, bubbly annular flow and droplet annular flow

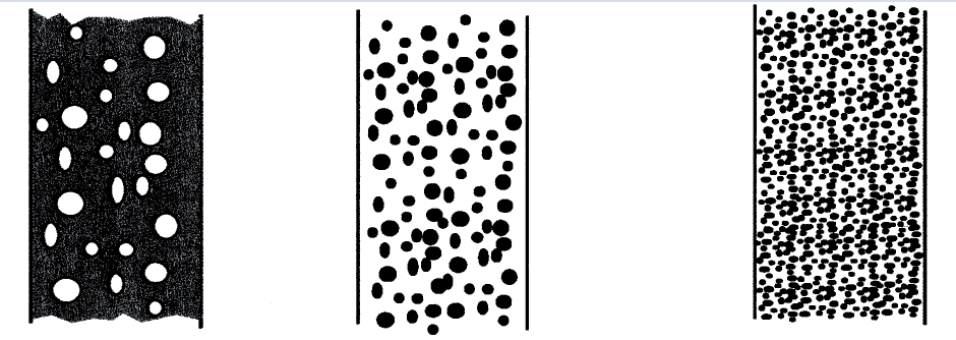

Figure B1 - 03 - Dispersed two-phase flows: bubbly flow, droplet flow and particulate flow

In separated two-phase flows, each phase plays a symmetrical role and the topology of the interface is not assumed. No hypothesis can be proposed for the shape of each phase and we cannot neglect the volume of one of the phases. There are two approaches for the mathematical description of such flows: either by tracking the interface between both fluids and solving Navier-Stokes equations in each one (Volume Of Fluid [16], Level-Set Methods [37]), or by using an averaging procedure to derive a set of conservation equations describing the two-phase flow as a whole and assuming that each phase may be simultaneously present at any point; in this second approach the smallest scales of the interface are not resolved but modelled, using the averaging procedure. The most well-known of these models is the Baer-Nunziato system of 7 equations [2], [34], but reduced models can also be used, as in [19], [24].

In the case of dispersed flows, one phase is assumed to be dilute (typical values of the volume fraction lie between 10^{-5} and 10^{-2}) and composed of spherical inclusions (droplets, particles or bubbles) dispersed inside the other phase (called the “carrier phase”). All inclusions are assumed to be very small compared to the macroscopic scale of the system and therefore can be considered as pointwise. Given this assumption the flow around and inside the particles does not have to be computed. The influence of the inclusions on the carrier phase is taken into account with the introduction of source terms in the right hand side of the Navier-Stokes equations.

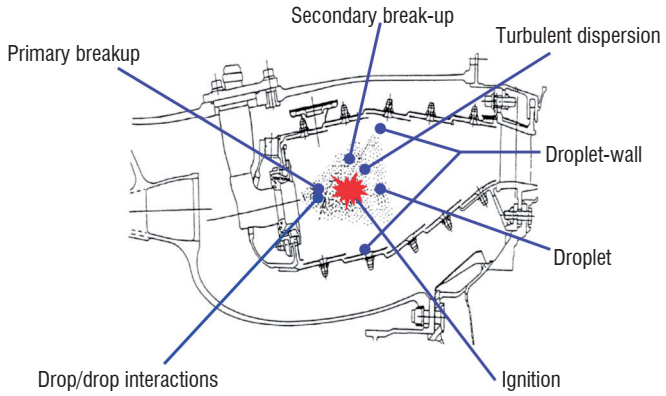

Figure 1 - Main physical phenomena occurring in the combustion chamber of a turbojet engine

In liquid fuel rocket engines, the simulation of the LOX/H2 cryogenic flame process needs both separated two-phase flow and dispersed two-phase flow descriptions (Figure 2).

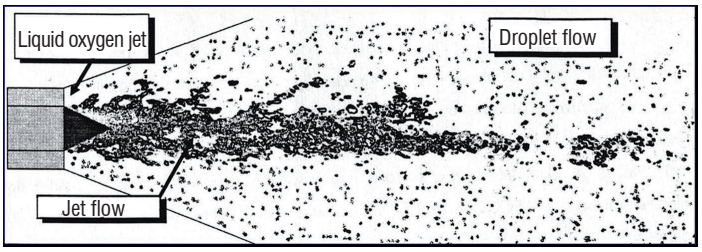

Figure 2 - Schematic representation of the turbulent reactive two-phase flow occurring in liquid fuel rocket engines. Atomization of the liquid oxygen jet, secondary breakup, evaporation and combustion

In solid propellant rockets, aluminum particles are used in order to increase the temperature of the burnt gases in the combustion chamber. When these particles burn, small alumina droplets are produced (from 1 μm to 100 μm) and convected out of the nozzle in the exhaust gases. Figure 3 represents the 2D-simulation of a small-scale rocket booster (LP6) fired at the Onera-Fauga center.

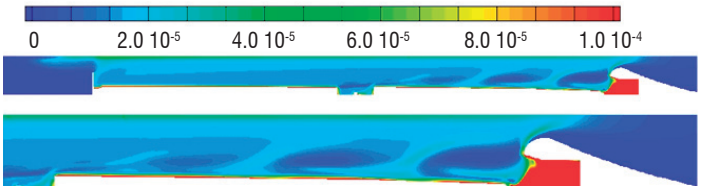

Figure 3 - LP6 solid propellant booster. Alumina droplet volume fraction field. Computation has been performed with CEDRE, using the SPIREE Eulerian solver

Gas-particle flows also play an important role in icing (Figure 4) and water ingestion phenomena (ingestion of hail, ice-crystals and rain drops in turbojet engines). For example ice accretion on aircraft is due to the presence of supercooled water droplets in the air, which may deposit or not on the aircraft surfaces depending on their size and relative velocity. SLD ice is ice formed in Supercooled Large Droplet (SLD) conditions. It is similar to clear ice, but because the droplet size is large it often extends to unprotected parts of the aircraft and forms larger ice shapes, and faster than normal icing.

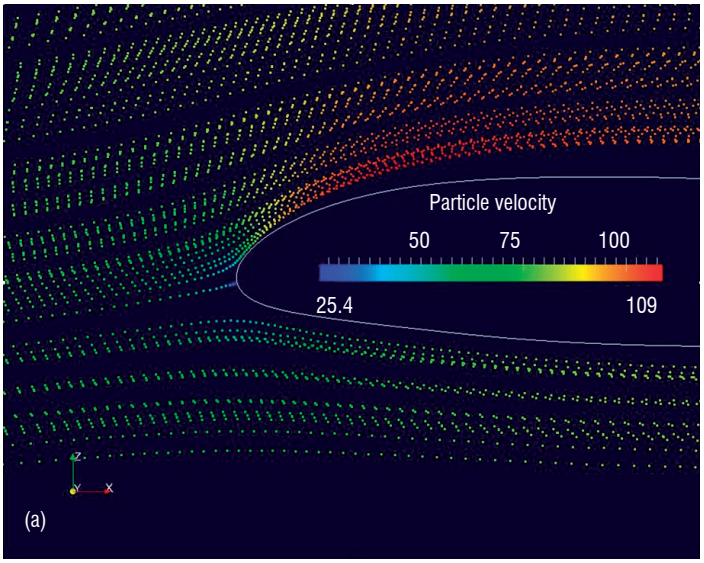

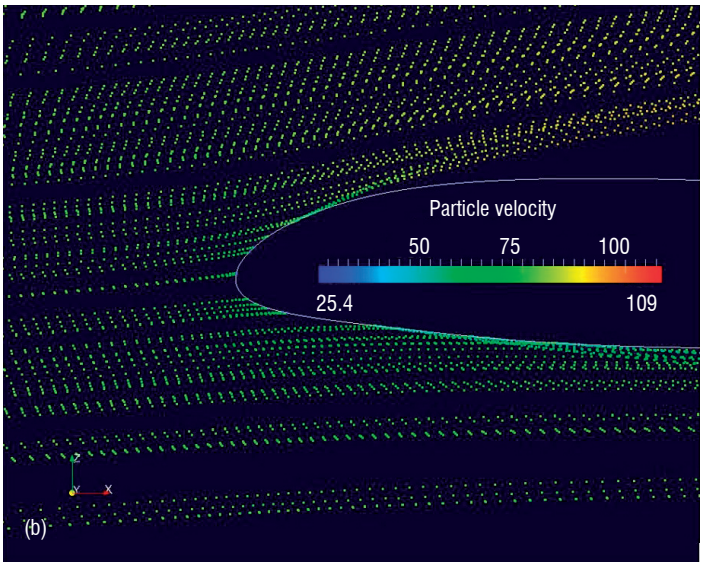

Figure 4 - Super-cooled water droplet trajectories around a NACA23012 airfoil. (a): Droplet diameter = 10.9 μm – (b): Droplet diameter = 70.7 μm. Both computations have been performed with CEDRE, using the SPARTE Lagrangian solver

These examples show the large variety of possible applications even if the paper is limited to dispersed two-phase flows in the aerospace context. In order to perform all these applications, ranging from Icing to Propulsion, detailed physical models as well as efficient and robust numerical methods are required. In the recent past a lot of work has been done, including the development of the CEDRE Multi-Physics Code. So this paper reviews, for dispersed two-phase flows, the physical and numerical methods to be found in the literature, and also those which are implemented in the Onera code. The paper also highlights the new objectives and future challenges we are expecting to tackle.

As regards the description of dispersed two-phase flows, two solvers have been implemented; the first, SPARTE, is based on a Lagrangian formulation while the second, SPIREE, is based on an Eulerian formulation. The drawbacks and advantages of each are discussed briefly in § Numerical methods (Box 2) but the best formulation often depends on the characteristics of the simulation. Our strategy is to use two solvers for the description of the dispersed phase. Our constant objective is to improve all the models and the numerical methods of

both the solvers in order to be able to run more and more complex industrial applications including Large Eddy Simulations (LES), Multi-Velocity Eulerian formulation, moving meshes, etc.

In the future, the major new challenge will be to develop the Multiphase solver and to realize a coupling with the "dispersed" two-phase flow solvers. The development of a Multiphase solver has been started recently, to describe "separated" and "mixed" two-phase flow, as shown in Box 1. With the strategy of coupling solvers we intend to realize complete simulation of, for example, liquid fuel rocket engines (Figure 2). The Multiphase solver will be used to describe the atomization of the liquid oxygen jet while the secondary break-up, evaporation and combustion will be simulated with SPIREE or SPARTE. The coupling strategy will have to be done very carefully as regards the physical modeling for transition as well as the numerical methods. Note that the main difficulty for spray computation is precisely the numerical simulation of the primary atomization process.

Other challenges are expected to be the coupling of the SPIREE and SPARTE solvers to take the major advantages of each formulation, coupling the same solver used with different physical or numerical methods (as in the RANS-LES computation), coupling SPIREE or SPARTE with the recently developed FILM solver [30] for film-particle interactions etc.

Gas-particle flow modeling

Williams "kinetic" equation

The modeling of dispersed two-phase flows is based on a mesoscopic description of the dispersed phase. Particles are assumed to be spherical and fully characterized by a small set of variables: position $\mathbf{x}$, radius r (or more generally a size variable denoted by φ), velocity $\mathbf{v}$ and temperature θ. In most applications, the particle number density function contains all the necessary information on the dispersed phase. By definition, $f(t,\mathbf{x},r,\mathbf{v},\theta)d\mathbf{x}drd\mathbf{v}d\theta$ denotes the averaged number of droplets with a size in $[r,r+dr]$, a velocity in $[\mathbf{v},\mathbf{v}+d\mathbf{v}]$, a temperature in $[\theta,\theta+d\theta]$ and located in the volume $[\mathbf{x},\mathbf{x}+d\mathbf{x}]$ at time t.

The following Boltzmann-like equation (introduced by Williams in [40] and [41]) expresses the conservation of the number density function (n.d.f) f in the phase space:

$$\frac{\partial f}{\partial t}+\nabla_{\mathbf{x}}\cdot(\mathbf{v}f)+\nabla_{\mathbf{v}}\cdot(\mathbf{F}f)+\frac{\partial}{\partial r}(Rf)+\frac{\partial}{\partial\theta}(Hf)=\Gamma+Q \qquad (1)$$

In this balance equation (1), the left-hand-side stands for the "transport" of the particles in the phase space ($\mathbf{F}$, R and H correspond respectively to the force acting on a particle, the evaporation rate and the heat exchange rate) while Γ and Q on the right-hand-side stand for the effect of fragmentation and collision phenomena respectively. Note that $\mathbf{F}$, R and H depend on the local gas composition, velocity and temperature.

Modeling of microscale physical phenomena in gas-particle flows

Force acting on a particle

In the most general case the total force includes contributions from drag, gravity, lift, added mass effect, pressure gradient and viscous stresses (Basset). In the following equation, $m=(4/3)\pi r^3\rho_p$ denotes the particle mass, ρ stands for the fluid density while ρ_p stands for the particle density. Vector $\mathbf{u}$ represents the fluid velocity and $D\mathbf{u}/Dt$ its material derivative along the trajectory.

$$m\frac{d\mathbf{v}}{dt}=\mathbf{F}_D+m\mathbf{g}+\mathbf{F}_L+\rho C_m\frac{\pi d^3}{6}\left(\frac{D\mathbf{u}}{Dt}-\frac{d\mathbf{v}}{dt}\right)-\rho\frac{\pi d^3}{6}\nabla p+\mathbf{F}_B \qquad (2)$$

The first term on the right hand side of the equation (2) is the drag force $\mathbf{F}_D$. The second term on the right hand side is the gravitational force. The remaining terms in equation (2) correspond to the lift force, added mass effect, pressure gradient term and Basset force. The added mass coefficient C_m is in general constant, equal to the inviscid approximation: $C_m=0.5$ (see for instance [6]). The lift mechanism $\mathbf{F}_L$ considers the velocity gradient around a particle moving in a non-uniform rotational flow [33]. The pressure gradient term is responsible for the buoyancy force and the Basset term, also called the history term, is due to the combination of viscous forces and particle acceleration with respect to the carrier flow.

Fortunately, including all these forces in the particle motion equation is not really necessary for aerospace applications. Because of the very high density of the particulate phase compared to the fluid phase ($\rho/\rho_p\approx10^{-3}$), the only external forces to be accounted for are the drag force and the force of gravity. The general expression of the drag force reads:

$$\mathbf{F}_D=\frac{1}{2}\rho C_D\pi r^2(\mathbf{u}-\mathbf{v})\|\mathbf{u}-\mathbf{v}\| \qquad (3)$$

where C_D is the drag coefficient depending on the particle radius as well as on the characteristic of the fluid flow around the particle. The dynamic relaxation time is written $\tau_v=(8\rho_p r)/(3C_D\rho\|\mathbf{u}-\mathbf{v}\|)$. This velocity response time represents the time required for a particle to respond to a change in the fluid velocity.

Evaporation phenomena and heat transfer

A large variety of models are available for the description of mass and heat transfer between the particles and the gas. The simplest one is based on the d^2 law [36]. In this model the droplet temperature is assumed to be constant and droplet heating is neglected. A linear regression in time for the droplet surface is then obtained. At the other extreme, much more complex models, taking into account the change in temperature profile inside the droplet, give a very accurate description of the evolution of the droplet surface temperature.

A classic intermediate model, resolving droplet heating but still not resolving internal conduction, is the infinite conductivity model. The droplet temperature is assumed to be uniform but varies with time. Such a model can be found in [1]. This evaporation model is used in the SPIREE and SPARTE solvers. The variation of the droplet surface $\varphi=S$ obeys:

$$\dot{S}=\frac{dS}{dt}=-4\pi\frac{Sh^*\langle\rho D\rangle}{\rho_p}\ln[1+B_M] \qquad B_M=\frac{Y_s-Y_\infty}{1-Y_s} \qquad (4)$$

This expression of dS/dt is derived from the mass conservation equations for the vapor and the gas mixture under the assumption that the gas-flow around the droplet is stationary. The parameter B_M stands for the Spalding dimensionless mass transfer number. To take into account the effect of the convective transport on vaporization due to the droplet motion relative to the gas it is the so-called "film theory" that is used and the convective Sherwood number Sh is introduced. This number has to be modified ($Sh^*=2+(Sh-2)/F_M(B_M)$) to take

the presence of the Stefan flow into account. Note that the subscripts s,∞ refer to the conditions at the droplet surface and at infinity from the droplet surface, e.g. in the external gas flow, and $\langle . \rangle$ represents an averaged value between conditions s,∞. D,Y stand, respectively, for the binary diffusion coefficient and the vapor mass fraction in the gas.

Then, if we examine the energy conservation equation, we can deduce the evolution for H which corresponds to the heat flux entering the droplet. The equation is written:

$$mc_p H = mc_p \frac{d\theta}{dt} = \lambda \pi 2 r N u^* (T-\theta) + L_v(T_s)\dot{m} \qquad (5)$$

In this last equation (5), a part of the flux $L_v(T_s)\dot{m}$ serves for vaporization. Note that $L_v(T_s)$ represents the latent heat of vaporization at temperature T_s and $\dot{m} = -\left(\rho_p \sqrt{S}\right)/\left(4\sqrt{\pi}\right)\dot{S}$ is the instantaneous vaporization rate. The other part $\lambda \pi 2 r N u^* (T-\theta)$ in equation (5) serves for heating-up the droplet. Note that only the convective heat transfer (or thermal conduction) is considered around the particle. As a consequence, the expression for heat exchange between particle and fluid is given by a conductive flux possibly modified by convective effects where we have introduced Nu^* for the convective Nusselt number.

Droplet secondary break-up

Secondary break-up is the name given to the fragmentation of a droplet under the action of the pressure and shear forces exerted by the gas on the droplet surface. This phenomenon can only occur if the relative velocity between the gas and the droplet is greater than a critical value. In dimensionless form, this threshold condition can be written: $\mathrm{We} > \mathrm{We}_c$, where We denotes the Weber number (defined below) and We_c its critical value ($\mathrm{We}_c \approx 12$). As shown in Figure 5, secondary break-up is a very complex multi-scale phenomenon which cannot be modeled in detail but rather from a statistical point of view and using experimental results.

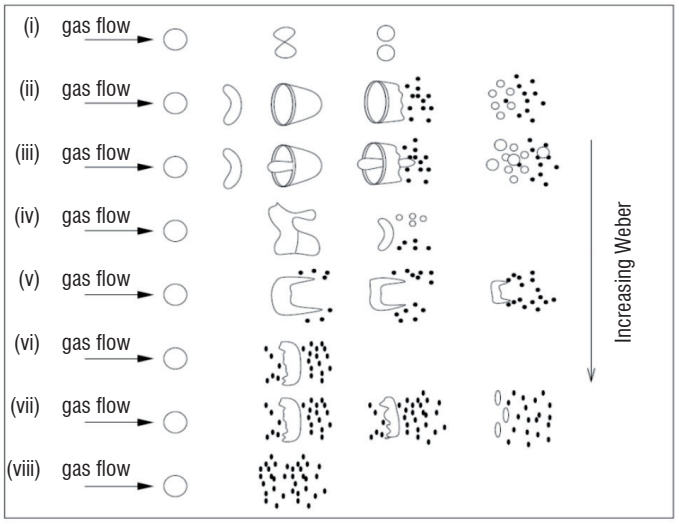

Figure 5 - Secondary break-up regimes depending on the value of the Weber number

The general form of the fragmentation (or secondary break-up) term of (1) reads as follows:

$$\Gamma(f)(\mathbf{v},r) = -\nu_{bup}(\mathbf{v},r) f(\mathbf{v},r) + \int_{\mathbf{R}^+}\int_{\mathbf{R}^3} \nu_{bup}(\mathbf{v}^*,r^*) h_{bup}(\mathbf{v},r,\mathbf{v}^*,r^*) f(\mathbf{v}^*,r^*) d\mathbf{v}^* dr^* \qquad (6)$$

where $\nu_{bup}(\mathbf{v},r)$ denotes the breakup frequency. In SPARTE (see § Numerical Methods and Applications of the present paper) it is given by the following model, with σ denoting the surface tension coefficient and τ_{bup} corresponding to the average break-up time:

$$\nu_{bup}(\mathrm{v},r) = \begin{cases} 0 & \text{if } We \le We_c \\ \dfrac{1}{\tau_{bup}(v,r)} \approx \dfrac{1}{5}\sqrt{\dfrac{\rho_g}{\rho_p}}\dfrac{\left\|\mathrm{v}-\mathrm{U}_g\right\|}{2r} & \text{if } We > We_c \end{cases} \qquad (7)$$

$$\text{where : } We = \frac{2r\rho_g \left\|\mathrm{v}-\mathrm{U}_g\right\|}{\sigma}$$

We refer to [17] for the expression of the function h_{bup} which represents the p.d.f. (probability density function) of the droplets produced by the fragmentation of a given droplet of radius r^* and velocity $\mathbf{v}^*$.

Collision

Collisions occur if the dispersed phase is dense enough and if the relative velocity between particles is not too small. In the case of solid particles, collisions can only modify particle velocities but in the case of droplets both size and velocity may change and the outcome of a collision is much more complex: several regimes can be observed as depicted in Figure 6.

Collision modeling is very complex for both solid and liquid particles. A large number of studies have been devoted to this topic during the three last decades and it is not possible to summarize them all in this introductory paper. We refer for example to the work of Rabe [29] for droplet collision and Février [12] for the case of solid particles.

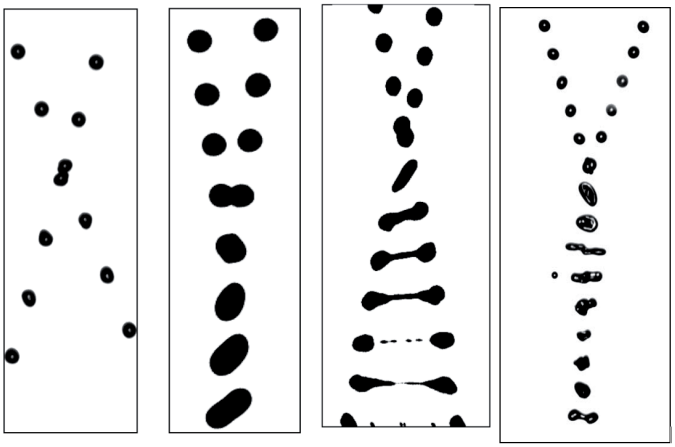

Figure 6 - Droplet collision regimes. From left to right: bouncing, coalescence, stretching separation, reflexive separation

Here, for the sake of completeness, we only give the general form of the collision term which can be used to take droplet coalescence into account:

$$\begin{aligned} Q(f)(\mathbf{v},r) = & -\int_{\mathbb{R}^+}\int_{\mathbb{R}^3} \pi\left(r+r^*\right)^2 \left\|\mathbf{v}-\mathbf{v}^*\right\| E_{coll}(r,r^*,\mathbf{v},\mathbf{v}^*) \\ & E_{coal}(r,r^*,\mathbf{v},\mathbf{v}^*) f(\mathbf{v},r) f(\mathbf{v}^*,r^*) d\mathbf{v}^* dr^* \\ & + \frac{1}{2}\int_{\mathbb{R}^+}\int_{\mathbb{R}^3} \pi\left(r^{\%}+r^*\right)^2 \left[\frac{r}{r^{\%}}\right]^{11} \left\|\mathbf{v}^{\%}-\mathbf{v}^*\right\| E_{coll}(r^{\%},r^*,\mathbf{v}^{\%},\mathbf{v}^*) \\ & E_{coal}(r^{\%},r^*,\mathbf{v}^{\%},\mathbf{v}^*) f(\mathbf{v}^{\%},r^{\%}) f(\mathbf{v}^*,r^*) d\mathbf{v}^* dr^* \end{aligned} \qquad (8)$$

with E_{coll} being the collision efficiency and E_{coal} the coalescence efficiency [39] and

$$\begin{cases} r^3 = (r^{\%})^3 + (r^*)^3 \\ r^3\mathbf{v} = (r^{\%})^3\mathbf{v}^{\%} + (r^*)^3\mathbf{v}^* \end{cases} \quad (9)$$

This last equation simply corresponds to the conservation of mass and momentum during the coalescence process.

Particle – wall interactions

Particle-wall interactions are of major importance for many physical or industrial processes involving gas-particle flows (spray cooling, rain and hail ingestion in turbojet engines, icing, erosion, etc.). The outcome of a particle impact on a solid wall depends on a number of parameters: particle-wall relative velocity, particle diameter, particle temperature, wall temperature, wall roughness, etc., and several interaction regimes can be experimentally observed: bouncing, splashing (or fragmentation) with partial depositing and secondary particle emission, full depositing. The description and the modeling of these complex phenomena is beyond the scope of this article and we refer to [14], amongst others, for more details.

Fluid models

All fluid models for gas-particle flows are based on conservation equations for some particular moments of the number density function. These models can be formally derived from the kinetic equation (1) by assuming particular closure assumptions.

Let us first introduce the following notations:

$$\bar{n}(t,\mathbf{x},r) = \iint_{\mathbf{v},\theta} f(t,\mathbf{x},r,\mathbf{v},\theta)d\mathbf{v}d\theta$$

$$\bar{n}\,\bar{\rho}(t,\mathbf{x},r) = \iint_{\mathbf{v},\theta} f(t,\mathbf{x},r,\mathbf{v},\theta)\rho(\theta)d\mathbf{v}d\theta$$

$$\bar{n}\,\bar{\rho}(t,\mathbf{x},r)\bar{\mathbf{v}}(t,\mathbf{x},r) = \iint_{\mathbf{v},\theta} f(t,\mathbf{x},r,\mathbf{v},\theta)\rho(\theta)\mathbf{v}d\mathbf{v}d\theta$$

$$\bar{n}\,\bar{\rho}(t,\mathbf{x},r)\bar{h}(t,\mathbf{x},r) = \iint_{\mathbf{v},\theta} f(t,\mathbf{x},r,\mathbf{v},\theta)\rho(\theta)h(\theta)d\mathbf{v}d\theta$$

where h stands for the particle enthalpy. Integrating the "kinetic" equation (1) with respect to θ and $\mathbf{v}$, and using conventional notations, we formally get a system of balance equations of the following form:

$$\begin{cases} \dfrac{\partial}{\partial t}\bar{n} + \nabla_{\mathbf{x}}\cdot\left(\bar{n}\bar{\mathbf{v}}\right) + \dfrac{\partial}{\partial r}\left(\bar{n}\bar{R}\right) = \Gamma^1 + Q^1 \\ \dfrac{\partial}{\partial t}\left(\bar{n}\bar{\rho}\right) + \nabla_{\mathbf{x}}\cdot\left(\bar{n}\bar{\rho}\bar{\mathbf{v}}\right) + \dfrac{\partial}{\partial r}\left(\bar{n}\bar{\rho}\bar{R}\right) = \Gamma^2 + Q^2 \\ \dfrac{\partial}{\partial t}\left(\bar{n}\bar{\rho}\bar{\mathbf{v}}\right) + \nabla_{\mathbf{x}}\cdot\left(\bar{n}\bar{\rho}\bar{\mathbf{v}}\otimes\bar{\mathbf{v}} + P\right) + \dfrac{\partial}{\partial r}\left(\bar{n}\bar{\rho}\bar{R}\bar{\mathbf{v}}\right) - \bar{n}\bar{\rho}\bar{\mathbf{F}} = \Gamma^3 + Q^3 \\ \dfrac{\partial}{\partial t}\left(\bar{n}\bar{\rho}\bar{h}\right) + \nabla_{\mathbf{x}}\cdot\left(\bar{n}\bar{\rho}\bar{h}\bar{\mathbf{v}}\right) + \dfrac{\partial}{\partial r}\left(\bar{n}\bar{\rho}\bar{R}\bar{h}\right) - \bar{n}\bar{\rho}\bar{c}_p\bar{H} = \Gamma^4 + Q^4 \end{cases} \quad (10)$$

The term P stands for the second order kinetic stress tensor (equivalent to a generalized pressure tensor). It is due to the dispersion of the droplet velocity distribution function. It reads:

$$P(t,\mathbf{x},r) = \iint_{\mathbf{v},\theta}\rho(\theta)\left(\mathbf{v}-\bar{\mathbf{v}}\right)\otimes\left(\mathbf{v}-\bar{\mathbf{v}}\right)f(t,\mathbf{x},r,\mathbf{v},\theta)d\mathbf{v}d\theta \quad (11)$$

In the simplest (and widely used) class of models, this last term is simply neglected which may lead to some anomalous behavior. More complex fluid models can also be used in which P is not eliminated but deduced from the resolution of additional transport equations for higher order moments of f. The description of these models is beyond the scope of this paper and we refer the reader to [35], [13], [8], [21] amongst others.

The last step to get a fluid model for the particulate phase consists in eliminating the size variable r and several options are possible. The first option leads to a two-fluid model which can be derived from the kinetic equation (1) if we proceed to an integration over the whole phase space. The information on size dispersion is lost in this derivation. The two-fluid model consists in solving an averaged description of the spray. As a consequence, the polydispersed characteristic of the spray cannot be taken into account and this limitation is a real drawback.

A second option is the sampling method in which the presumed n.d.f (number density function) is written under a sum of Dirac mass with respect to the size variable as depicted on the left hand side of Figure 7. The system for each sample is derived from the kinetic equation with the same assumptions as for the two-fluid model. The sampling method thus leads to N systems similar to system (10). As a consequence there is no interaction terms between particles of different sizes and complex phenomena such as coalescence or secondary break-up are difficult to handle in this framework. On the other hand, sampling models are very easy to implement.

Finally, the last option, often called the "multi-fluid" model or sectional model (see for instance [20], [10]), is illustrated on the right hand side of Figure 7. It has been introduced in [15]. Information on the droplet size distribution is kept at the macroscopic level thanks to a finite volume discretization with respect to the size variable. A set of equations is derived for each section and, in this type of model, sections are coupled thanks to mass, momentum and heat fluxes due to the finite volume approximation. More complex phenomena such as coalescence and fragmentation can also be easily included. The choice between first or second order is a compromise between precision of the phenomena description and the cost of the algorithms. The work presented in [9] provides some conclusions for the optimization in solid propellant combustion.

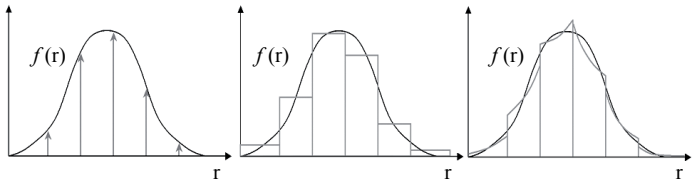

Figure 7 - Discretization of the droplet size distribution function in the sampling method (left), in the first order sectional approach (middle) and the second order sectional approach (right)

Numerical Methods

Introduction

The most direct numerical approach would consist in tracking all the particles present in the flow and to compute their changes individually. In such a method, each numerical particle would represent a given physical particle (or droplet). In the following, we shall refer to this method as the Discrete Particle Simulation method (DPS). For industrial applications,

this method cannot be applied because of the excessively large number of particles per unit volume and other approaches have to be used, which are based either on the discretization of the kinetic equation (1) or on the discretization of conservation equations derived from the kinetic equation. Three classes of methods may be used.

The first is the class of the so called “full spray equation methods”. These methods solve equation (1) directly by applying a finite volume or a finite difference method. But for realistic configurations, these methods are prohibited because of the high dimension number of the phase space (at least 8 in 3D).

The second is the class of Particle Methods or more generally Stochastic Particle Methods, which are also often called Lagrangian methods or Stochastic parcel methods [32]. From a physical point of view, they can be seen as a coarser version of the Discrete Particle Simulation method in which each “numerical particle” represents more than one physical particle. From a mathematical point of view, this class of methods can be interpreted as numerical methods for the direct resolution of the kinetic equation. These methods are described in section "Lagrangian methods".

The last class of method represents all numerical methods based on “fluid models” (set of conservation equations) derived from the kinetic equation. These methods generally based on a finite volume framework are often called Eulerian methods and are described in section "Eulerian methods".

Lagrangian methods

Particle methods (or stochastic particle methods) are commonly used for the calculation of polydisperse sprays in various application fields (see for example [28], [11], [32] and the references therein). A complete exposition of the derivation and the implementation of such a method is beyond of the scope of this paper. We refer, for example, to [17] or for details. Here, for the sake of completeness, we present the only main features of such a numerical method.

A particle method can be interpreted as a discretization method for the kinetic equation (1). The distribution function f at time t is approximated by a weighted sum of Dirac masses, $f_N(t)$, which reads:

$$f_N(t) = \sum_{i=1....N} w_i(t)\delta_{\mathbf{x}-\mathbf{x_i}(t)} \otimes \delta_{\mathbf{v}-\mathbf{v_i}(t)} \otimes \delta_{r-r_i(t)} \otimes \delta_{\theta-\theta_i(t)} \qquad (12)$$

Each weighted Dirac mass is generally called a ‘‘parcel’’ or “numerical particle” and can be physically interpreted as an aggregated number of real particles (or droplets, according to the context) located around the same point x_i, with the same velocity v_i, the same radius r_i and the same temperature θ_i. The weight w_i can be interpreted as the number of real particles associated with parcel i and N denotes the total number of parcels used in the computation.

Each time step of the numerical procedure is divided into 3 stages. The first one is devoted to the discretization of the l.h.s. of the kinetic Equation (1), modeling motion, heating and evaporation of the particles. The last two stages of a time step are devoted to the discretization of the collision and fragmentation operators.

Transport step

Several numerical schemes can be used according to the desired accuracy and numerical stability constraint. In SPARTE, the new position, velocity, temperature and radius of each numerical particle are calculated according to the following scheme:

$$\begin{cases} \mathbf{x_i^{n+1}} = \mathbf{x_i^n} + \mathbf{U}_g(t^n, \mathbf{x_i^n})\Delta t \\ \qquad + \left[\mathbf{v_i^n} - \mathbf{U}_g(t^n, \mathbf{x_i^n})\right](1-\alpha_i^n)\tau_p^n \\ \qquad + \left[\Delta t - (1-\alpha_i^n)\tau_p^n\right]\tau_p^n \mathbf{g} \\ \mathbf{v_i^{n+1}} = \mathbf{U}_g(t^n, \mathbf{x_i^n}) + \alpha_i^n\left[\mathbf{v_i^n} - \mathbf{U}_g(t^n, \mathbf{x_i^n})\right] \\ \qquad + (1-\alpha_i^n)\tau_p^n \mathbf{g} \\ \theta_i^{n+1} = \left(T^*\right)_i^n + \beta_i^n\left[\theta_i^n - \left(T^*\right)_i^n\right] \\ r_i^{n+1} = \left[\dfrac{\rho_p(\theta_i^n)}{\rho_p(\theta_i^{n+1})}\right]^{1/3} \\ \qquad \times \sqrt{\max\left[(r_i^n)^2 - \Delta t K_{ev}(r_i^n, \theta_i^n, \mathbf{x_i^n}, \mathbf{v_i^n}), 0\right)} \end{cases} \qquad (13)$$

where τ_p denotes the particle dynamical response time, τ_c the heat exchange response time (derived from equation (5)), T^* stands for the equilibrium temperature (depending on the gas temperature and the saturation temperature according to equation (5)) and $\mathrm{U}_g(t^n, x_i^n)$ stands for the gas velocity at the particle location and:

$$\alpha_i^n = \exp\left(-\frac{\Delta t}{\tau_p^n}\right) \qquad \beta_i^n = \exp\left(-\frac{\Delta t}{\tau_c^n}\right) \qquad (14)$$

This is an unconditionally stable first order scheme. Higher order explicit schemes (like Runge-Kutta schemes) can also be used but they are only conditionally stable and their stability condition is very constraining for small particles (because τ_p and $\tau_c \to 0$).

It is worth mentioning that particle-wall interactions are also taken into account during the transport step. Monte-Carlo algorithms are generally used to treat complex phenomena like splashing or bouncing on a rough wall to avoid the creation of a lot of new numerical particles.

Collision step

Several Monte-Carlo algorithms have been proposed in the literature for the treatment of droplet (or solid particle) collisions. They are inspired by methods used in molecular gas dynamics. They suppose that the computational domain is divided into cells, or control volumes, which are small enough to assume that the droplet distribution function is almost uniform over them. The algorithm used in SPARTE [17],[20] is close to the one proposed by O’Rourke [28]. In the case of droplets, it consists of the following three steps:

i) For each computational cell C_j, containing N_j parcels randomly choose $N_j/2$ pairs of parcels ($(N_j-1)/2$ if N_j is odd);

ii) For each pair p, let p_1 and p_2 denote the two corresponding parcels with the convention $w_1 \geq w_2$, where w_1 and w_2 denote the parcel weights; then for each pair p, randomly choose an integer v_p according to the Poisson distribution law:

$P(\nu) = \frac{\lambda_{12}^{\nu}}{\nu!}\exp(-\lambda_{12})$ with:

$$\lambda_{12} = \pi E_{coll} E_{coal} \frac{w_1 (N_J - 1)\Delta t}{vol(C_j)} (r_1 + r_2)^2 \left\| \mathbf{v}_1 - \mathbf{v}_2 \right\|$$

with $vol(C_j)$ being the volume of cell C_j, E_{coll} the collision efficiency, E_{coal} the probability of coalescence given that the collision has occurred and r_1, r_2 being the radii of parcels p_1, p_2. λ_{12} represents the average number of coalescences during $(N_j - 1)$ time steps between a given droplet of parcel p_2 and any droplet of parcel p_1; this is in accordance with the fact that a given pair of parcels is chosen on average every $(N_1 - 1)$ time steps.

iii) If $\nu_p = 0$, no coalescence occurs during this time step between the parcels p_1 and p_2. Otherwise, if $\nu_p > 0$, parcel p^1 undergoes ν_p coalescences with parcel p^2 and the outcome of the collision is treated as follows: first the weight w_1 of parcel p_1 is replaced by $w_1' = w_1 - \nu_p w_2$ and its other characteristics are left unchanged. If $w_1' < 0$ then parcel p_1 is removed from the calculation; secondly, the velocity v_2 and radius r_2 of parcel p_2 are updated according to:

$$r_2' = \left(r_2^3 + \nu_p r_1^3\right)^{1/3} \qquad \mathbf{v}_2' = \frac{r_2^3 \mathbf{v}_2 + \nu_p r_1^3 \mathbf{v}_1}{r_2^3 + \nu_p r_1^3}$$

and its weight w_2, is left unchanged.

Remarks

- This algorithm allows us to take into account several collisions between two given parcels during the same time step; this is an important feature to avoid a very restrictive condition on the time step. Nevertheless, to maintain good accuracy the time step Δt must be chosen small enough to ensure that the average number of collisions between two given parcels, p_1 and p_2, is such that : $\nu_p \; w_2 < w_1$.
- Other collision regimes (stretching or reflexive separation, bouncing, etc.) can also be taken into account by slightly modifying this algorithm.

Fragmentation step (only for droplets)

Monte-Carlo algorithms must also be used during this stage to avoid the creation of too many new numerical particles. The algorithm used in SPARTE reads as follows:

i) For each numerical particle in the computational domain, compute the Weber number defined as:

$$We_i^n = \frac{2\rho_g(t^n, \mathbf{x}_i^n) \left\| \mathbf{v}_\mathbf{i}^\mathbf{n} - \mathbf{U}_g(t^n, \mathbf{x}_i^n) \right\|^2 r_i^n}{\sigma}$$

ii) If $We_i^n > We^*$ (critical Weber number), then compute the particle fragmentation probability during the current time step :

$$\pi_i = 1 - \exp(-\frac{\Delta t}{\tau_i^{bup}})$$

where τ_i^{bup} denotes the average break-up time of the particle.

iii) Choose a random number α between 0 and 1 ; if $\alpha < \pi_i$ then fragmentation of the ith particle is considered to occur during the current time step and new numerical particles are created. The radius of each new particle is randomly chosen according to the model used for the p.d.f. h_{bup} of the resulting droplets. The number of "child" numerical particles is usually chosen between 1 and 5 to ensure a good compromise between accuracy and computational cost.

Additional remarks

- For dilute stationary two-phase flows, a variant of the particle method described above can be used. It is based on the following approximation of the stationary droplet density function:

$$f_N(\mathbf{x}, \mathbf{v}, r, \theta) = \sum_{i=1....N} \int_0^T \left[\dot{w}_i(t) \delta_{\mathbf{x}-\mathbf{x_i}(t)} \otimes \delta_{\mathbf{v}-\mathbf{v_i}(t)} \otimes \delta_{r-r_i(t)} \otimes \delta_{\theta-\theta_i(t)} \right] dt \quad (15)$$

where T stands for the maximum residence time of a particle in the system and where $\dot{w}_i$ stands for the number of particles carried along the ith numerical trajectory per unit time (particle number flow rate). From a practical point of view, calculating a macroscopic property of the dispersed phase in a given cell C of the mesh consists in computing an average over all the numerical particles pondered by their residence time in the cell C. Particle collisions cannot be taken into account but transport and fragmentation steps are treated in exactly the same way as for the unsteady particle method.

- For dense two-phase flows or combustion phenomena, influence of the dispersed phase on the gas flow has to be accounted for. Within the framework of the Lagrangian approach, source terms are easily calculated by summing the contribution of each numerical particle. An underrelaxation procedure can be applied (as in SPARTE for example) to avoid numerical instabilities when the coupling between both phases is strong and the time step between two successive exchanges is too large.

Eulerian methods

Given the conservation form of the equations, the finite volume method is the most natural candidate for discretization of fluid models but finite difference or finite element methods could also be used. In this article we focus on the finite volume scheme implemented into the SPIREE solver, included in CEDRE. Let $\mathbf{q}$ be the set of conservative variables. It can be a set of only 4 variables in the case of the 1D two-fluid model or a set of 6N variables in the case of the 3D polydisperse spray model with a sampling method or a sectional method (with N being the number of classes or sections). In terms of conservative variables $\mathbf{q} = (n, \rho, \rho\mathbf{v}, \rho e)$ for each class (sampling method) or section (sectional approach), and the system of equations can be formally written:

$$\begin{cases} \dfrac{\partial n}{\partial t} + div(n\mathbf{v}) = S^1 \\ \dfrac{\partial \rho}{\partial t} + div(\rho\mathbf{v}) = S^2 \\ \dfrac{\partial \rho\mathbf{v}}{\partial t} + div(\rho\mathbf{v} \otimes \mathbf{v}) = S^3 \\ \dfrac{\partial \rho e}{\partial t} + div(\rho e\mathbf{v}) = S^4 \end{cases} \quad (16)$$

A class or a section of droplets is defined by its density ρ_0 which depends on the temperature, by its diameter $d = 2r$, by a unique velocity $\mathbf{v}$ and by the specific total energy $e = \varepsilon + \|\mathbf{u}\|^2 / 2$ where the internal energy is given by $\varepsilon = \varepsilon_{ref} + c_p(T)\left[T - T_{ref}\right]$. An important parameter of the flow is the volume fraction α which can be linked to the other variables by $\alpha = n\pi d^3 / 6$ or $\rho = \alpha\rho_0$. Denoting by $\mathbf{q}_i^n, \mathbf{q}_j^n$

the vector of the conservative variables in cells i,j of the mesh and using conventional notations, the general form of a linearized implicit finite volume scheme reads:

$$\begin{cases} V_i \dfrac{\mathbf{q}_i^{n+1}-\mathbf{q}_i^n}{\Delta t} = \\ -\displaystyle\sum_{j\in v(i)} A_{ij} \left[\begin{array}{r} \psi(\mathbf{q}_i^n,\mathbf{q}_j^n) + \dfrac{\partial \psi(\mathbf{q}_i,\mathbf{q}_j)}{\partial \mathbf{q}_i}(\mathbf{q}_i^n,\mathbf{q}_j^n)(\mathbf{q}_i^{n+1}-\mathbf{q}_i^n) \\ + \dfrac{\partial \psi(\mathbf{q}_i,\mathbf{q}_j)}{\partial \mathbf{q}_j}(\mathbf{q}_i^n,\mathbf{q}_j^n)(\mathbf{q}_j^{n+1}-\mathbf{q}_j^n) \end{array} \right] \\ +V_i \left[\mathbf{S}\left(\mathbf{q}_i^n\right) + \dfrac{\partial S(\mathbf{q}_i)}{\partial \mathbf{q}_i}(\mathbf{q}_i^n)(\mathbf{q}_i^{n+1}-\mathbf{q}_i^n) \right] \end{cases} \quad (17)$$

In this formula, $\psi(\mathbf{q}_i^n,\mathbf{q}_j^n)$ stands for the numerical flux at the interface between left and right states $\mathbf{q}_i^n,\mathbf{q}_j^n$ while $\mathbf{S}\left(\mathbf{q}_i^n\right)$ stands for the source terms due to the effect of drag force, mass and heat exchanges as well as particle interaction terms in the control volume V_i.

An inherent difficulty of Eulerian methods is the construction of the numerical flux $\psi(\mathbf{q}_i^n,\mathbf{q}_j^n)$. In the context of the generalized unstructured meshes used in CEDRE we have selected upwind schemes for numerical stability reasons. However, the convective part of the system is only weakly hyperbolic and we need special schemes rather than the conventional schemes used for Navier-Stokes equations. The numerical flux used in SPIREE reads:

$$\psi(\mathbf{q}_i,\mathbf{q}_j) = \frac{1}{2}\left(\mathbf{F}_i+\mathbf{F}_j\right) + \frac{1}{2}\left|\langle \mathbf{u}\cdot\mathbf{n}\rangle_{ij}\right|\left(\mathbf{q}_i-\mathbf{q}_j\right) \quad (18)$$

The corresponding expressions for the Jacobian matrices used in the above implicit scheme read:

$$\begin{cases} \dfrac{\partial \psi(\mathbf{q}_i,\mathbf{q}_j)}{\partial \mathbf{q}_i} = \dfrac{1}{2}\left(\langle \mathbf{u}\cdot\mathbf{n}\rangle_i + \left|\langle \mathbf{u}\cdot\mathbf{n}\rangle_{ij}\right|\right)\mathbf{I} \\ \dfrac{\partial \psi(\mathbf{q}_i,\mathbf{q}_j)}{\partial \mathbf{q}_j} = \dfrac{1}{2}\left(\langle \mathbf{u}\cdot\mathbf{n}\rangle_j - \left|\langle \mathbf{u}\cdot\mathbf{n}\rangle_{ij}\right|\right)\mathbf{I} \end{cases} \quad (19)$$

where $\mathbf{I}$ stands for the identity matrix, $\langle \mathbf{u}\cdot\mathbf{n}\rangle_i, \langle \mathbf{u}\cdot\mathbf{n}\rangle_j$ are respectively the left and right normal velocities and denotes $\langle \mathbf{u}\cdot\mathbf{n}\rangle_{ij}$ the arithmetic averaged normal velocity at the interface. Another scheme implemented into the SPIREE solver is a Godunov type scheme which is written:

$$\psi(\mathbf{q}_i,\mathbf{q}_j) = \frac{1}{2}\left(\mathbf{F}_i+\mathbf{F}_j\right) + \frac{1}{2}\left(\left|\langle \mathbf{u}\cdot\mathbf{n}\rangle_i\right|\mathbf{q}_i - \left|\langle \mathbf{u}\cdot\mathbf{n}\rangle_j\right|\mathbf{q}_j \right) \quad (20)$$

This last scheme is based on the resolution of the Riemann problem (see [7] for example) for the convective part of the particles system. To bypass the difficulty of delta-shocks, which can occur in such a system, other very efficient schemes can be used such as kinetic schemes [3] derived from the pressureless system of gas dynamics. Note that if we consider the special case of the delta-shocks in the Riemann problem (see for example [22]), the Godunov and kinetic type schemes are very similar.

To increase the order of accuracy of the scheme, we can change, in the definition of the numerical flux, the interface values $\mathbf{q}_i,\mathbf{q}_j$ by linearly reconstructed states according to a MUSCL (Monotonic Upwind Scheme for Conservation Laws) [38] procedure. Note that in SPIREE we choose to directly reconstruct the conservative variables

$$\mathbf{q}_{ij} = \mathbf{q}_i + \frac{1}{2}(\nabla q)_{ij}.\mathbf{ij} \text{ and } \mathbf{q}_{ji} = \mathbf{q}_j - \frac{1}{2}(\nabla q)_{ji}.\mathbf{ij}$$

The approximate gradients $(\nabla q)_{ij},(\nabla q)_{ji}$ are obtained using a combination of centered and fully upwind gradients. The scheme described above is not monotone. It can create extrema and unphysical solutions. To reduce oscillations in the solution, a slope limiting procedure is used. Time integration is based on both implicit and explicit Runge-Kutta type schemes.

Applications

In this part, we present a few numerical examples involving dispersed two-phase flows in the aerospace context. All simulations have been performed with CEDRE code using either its Lagrangian or Eulerian solver (SPARTE or SPIREE respectively). SPARTE and SPIREE are based on the models and numerical methods described above in sections 2 and 3. The detailed content of each solver in terms of available models and boundary conditions can be found in the specific paper devoted to CEDRE [30].

For icing applications, a Eulerian computation is presented in this section but it should be noted that a Lagrangian has also been suggested in the introduction for icing applications. In fact, if the droplets are large or if we need to compute very complex physical phenomena

Box 2 - Comparison of Eulerian and Lagrangian methods

This work has looked at a large variety of models as well as numerical methods. The choice for a model associated with a numerical method is a very difficult task which depends on the application.

As far as models are concerned, the sampling method is very closely associated with the complex description of heat and mass transfer but does not allow the computation of interaction terms. The sectional approach is more complex than the sampling method but gives a better description of the size dispersion of the spray. Moreover, the sectional approach allows the computation of thick spray with the possibility of dealing with interactions (coalescence - fragmentation). A common difficulty for both sampling and sectional methods is the "mono-kinetic" hypothesis which makes the treatment of cross trajectories impossible. Some solutions exist and need to be implemented in the code.

As regards numerical methods, Lagrangian methods seem very efficient and suitable for a good level of modelling. But Lagrangian methods can induce a very high cost of computation, e.g. unsteady cases. Eulerian methods seem more suitable for parallel computations and implicit algorithms but raise the problem of numerical diffusion, while the Lagrangian method means we have the difficulty of the coupling with a Eulerian resolution of the gas dynamics.

as wall-particles interactions, then the Lagrangian approach is very useful. But, if we want to try a 3D computation on an aircraft, the Eulerian approach is better. Note that a coupling of the two methods could be of great interest.

Concerning liquid propulsion and the MASCOTTE facility, the Lagrangian method has been used because we don't compute the primary atomization and the particles are directly injected into the volume according to experimental data. The life time of the particles is very short because of evaporation and the 3D computation is less costly. The Eulerian method could also have been used by changing the domain and having a new limit for fluxes particles injection. On the other hand, with the introduction of the multiphase solver in the code, we expect to be able to realize a fully 3D Eulerian of the MASCOTTE facility by coupling SPIREE with the new solver in order to obtain the size distribution of the spray by computing primary atomization.

Concerning solid propulsion, mentioned in the introduction, the surface injection of propergol is very large and the number of particles due to the combustion is very high. A Lagrangian computation would have been much more expensive than the Eulerian one so SPIREE has been chosen. Nevertheless, due to the high number of particles, interaction phenomena have to be taken into account, so the sophisticated sectional approach has to be used in this case if we want a precise simulation.

Icing applications

The experimental facility used is the PAG (Petit Anneau Givrant) located at CEPr (Centre d'Essais des Propulseurs). The model represents a three-dimensional helicopter air inlet and for this the entire wind tunnel section was modified as illustrated in Figure 8. The arrow symbolizes the air flow path, the up-stream section is a 20 cm square and the height of the removable wall is 10 cm in order to reach the maximum air velocity of 75 m.s^{-1} in this configuration. Two main impact zones have been characterized: the front quarter of the cylinder, instrumented with heater mats and temperature sensors, and the removable wall on the left hand side (Figure 8).

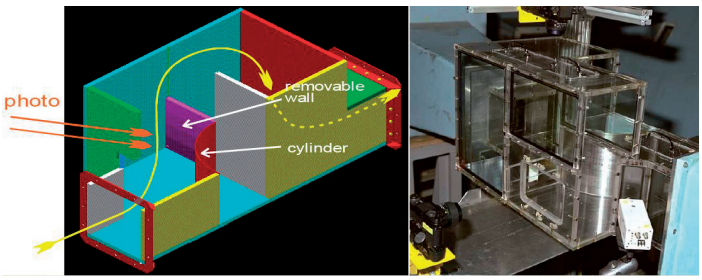

Figure 8 - Schematic representation view of the 3D duct

The Eulerian solver SPIREE is used as transport droplet module in the ONICE3D [23] Icing code developed at Onera. The problematic of degradation of performance in icing prediction is important and here we present one of the applications used to validate the Eulerian solver in the droplet capture process. Figure 9 (a) shows the numerical distribution of the water collection coefficient in the duct while in Figure 9 (b) we see the ice accreted on the cylinder in low temperature conditions (i.e. 243 K).Indeed, in low temperature cases, the droplets impinge and freeze immediately. So, the ice deposit is directly related to the water collection coefficient. The comparison shows a good agreement between experimental results and numerical simulations. These types of Icing problem simulations using SPIREE use the same strategy as in [5], [4], [42].

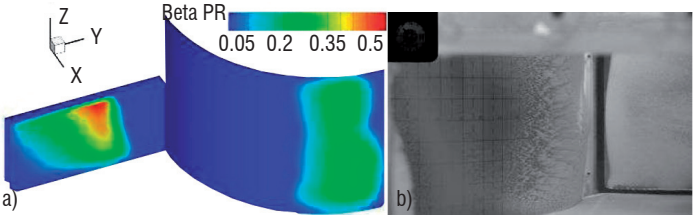

Figure 9 - Comparison between the Eulerian simulation of accretion and experiment

Liquid propulsion

The problem of high frequency combustion instabilities is a recurrent issue for liquid rocket engine propulsion. The origin of these instabilities is the coupling between acoustic and combustion processes such as atomization, vaporization and mixing. At Onera we are concentrating our efforts on the coupling between acoustics and vaporization. In order to study this difficult problem we have proceeded step by step, performing more and more complex simulations. For each step, the numerical results were compared to theoretical data or analytical solution. The first step was to study acoustic damping in a closed 1D cavity or equipped with a nozzle. We used the Eulerian solver for the second step simulation. This second step deals with the interaction between an acoustic wave and a suspension of inert particles in a closed 1D cavity. An exact solution of the problem can be computed in such a configuration and we have successfully compared simulation results and the theory on both the shift of the frequency and the damping of the oscillations. Figure 10 gives the change in frequency shift (or the damping) against $\omega_1\tau_u$ where ω_1 is the wave number without particles $\left(\omega_1 = \pi / L_{cavity}\right)$ and τ_u is the Stokes time which is proportional to the square of the particle diameter $\left(\tau_u = \rho_l d^2 / 18\mu\right)$.

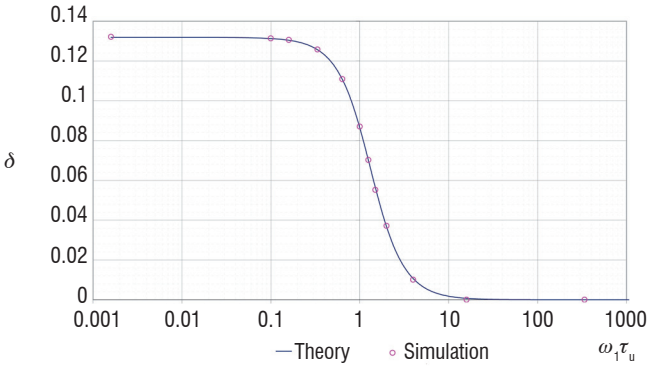

Figure 10 - Frequency shift

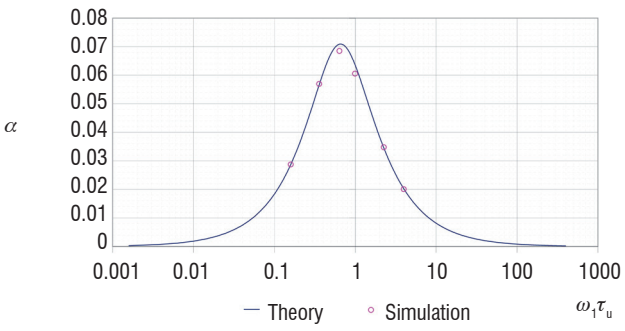

Figure 11 - Damping

Figures 12 and 13 below show another application of CEDRE related to the simulation of cryogenic propulsion. It corresponds to the simulation of an H2-O2 flame in the MASCOTTE facility at Onera Palaiseau. In this case the SPARTE Lagrangian solver has been used for the simulation of the liquid phase. In both calculations, the atomization process has not been simulated and oxygen droplets have been directly injected from a fictitious surface corresponding to the limit of the primary atomization zone. We refer to [25], [26] and [27] for all the details of these computations.

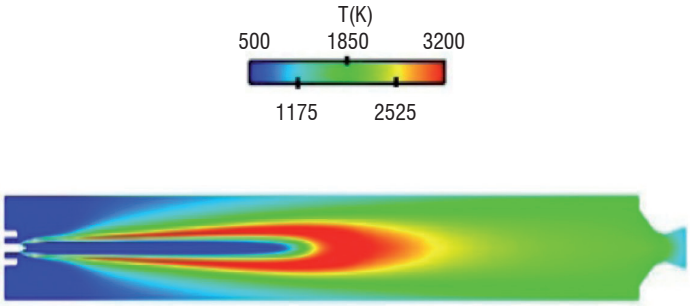

Figure 12 - 2D-RANS simulation of a GH2-LOx flame in the MASCOTTE Facility at P = 10 Bar – View of the temperature field inside the combustion chamber

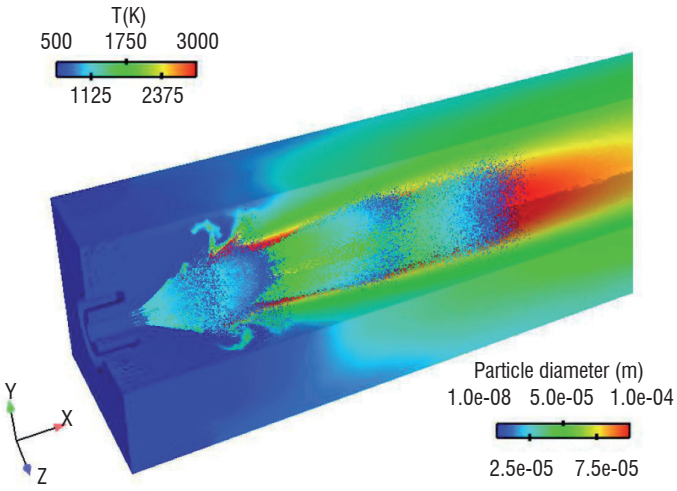

Figure 13 - 3D LES simulation of a GH2-LOx flame in the MASCOTTE Facility at P = 10 Bar – View of the temperature field and droplet position colored by their diameter

Conclusion

In this paper, we have given an overview of the models and numerical methods used for the simulation of dispersed two-phase flows. We have emphasized that both Eulerian and Lagrangian approaches can be related to a common underlying kinetic equation corresponding to a mesoscopic level of description.

The Lagrangian procedure treats the kinetic spray equation by solving the motion of a large number of numerical particles (parcels) in space, associated with variables of time, position and droplet velocity, size and temperature or other relevant quantities. The mean spray properties are obtained by averaging over a representative sample of parcels that cross a defined volume in a certain time interval. The main advantage of the Lagrangian procedure lies in its ability to reproduce spray physical behavior with a high degree of precision: a Lagrange computation with small sample volumes, short time intervals and a large number of parcels theoretically allows a detailed prediction of almost all physical phenomena occurring in an unsteady polydisperse spray flow.

However, the computational costs increase with the number of parcels and the problematic issue in the simulation of unsteady spray flows with Euler–Lagrange methods is the optimal choice for the injection frequency of new numerical particles (or the total number of simulated trajectories in the simulation of steady flows). We have to make sure that the numerical results do not depend on this parameter. It was also observed by Riber et al. [31] that the speedup of the Euler–Lagrange method by increasing the number of processors is not ideal because of the parallel load imbalance generated by the partitioning algorithm.

The Eulerian method consists in solving balance equations for various density fields of physical droplet quantities at each position and time. A finite volume discretization is generally applied. This formulation has the advantage of simplicity (the same kind of discrete equations for both phases) and the fact that, irrespective of the amount of droplets in a region, the same number of equations have always to be solved. Hence in Euler–Euler computations a cost is added for the dispersed phase which is independent of the mass loading. In consideration of these issues, we believe that the Eulerian procedure could be a good alternative for spray LES computations, in particular for computations of dense and unsteady particle flows using massively parallelized computers.

For the two last decades, thanks to the improvement of numerical models and the increase in computational power, the numerical simulation of dispersed two-phase flows has reached an advanced level of maturity. Using its two particulate phase solvers, CEDRE offers the possibility of performing such simulations for complex 3D industrial applications. However, several challenges are still to be met. For combustion applications, the main difficulty for spray computation is the numerical simulation of the primary atomization process and its coupling with dispersed flow solvers. Until now, droplets are directly injected at some given points in the computational domain and the droplet size and velocity distributions are chosen according to some experimental data. This procedure requires empirical data which is not always available and it is not appropriate for unsteady simulations (LES or URANS). Another very important problem for industrial applications concerns the modeling of spray – wall or spray – film interactions (icing problems, spray cooling, etc.). Some models are already implemented in SPARTE and SPIREE but they have still to be improved and coupled with the film solver of CEDRE. This work is currently in progress ■

References

[1] B. ABRAMZON and W.A. SIRIGNANO - *Droplet Vaporization Model for Spray Combustion Calculations*. International Journal of Heat and Mass Transfer, Vol. 32, n°9, pp. 160-1618 (1989).

[2] M.R. BAER, J.W. NUNZIATO - *A Two-phase Mixture Theory for the Deflagration-to-Detonation Transition (DDT) in Reactive Granular Materials*. Journal of Multiphase flows, 12, pp. 861-889 (1986).

[3] F. BOUCHUT, S. JIN and X. LI - *Numerical Approximation of Pressureless and Isothermal Gas Dynamics.* SIAM J. Num. Anal, 41, pp. 135-158 (2003).

[4] Y. BOURGAULT, Z. BOUTANIOS and W. HABASHI - *Three-Dimensional Eulerian Approach to Droplet Impingement Simulation Using FENSAP-IC*E, Part 1 : Model, Algorithm, and Validation. Journal of Aircraft, Vol. 37, n°1 (2000).

[5] Y. BOURGAULT, W. HABASHI, J. DOMPIERRE and G. BARUZZI - *A Finite Element Method Study of Eulerian Droplets Impingement Models.* International Journal for Numerical methods in fluids. 29, pp. 4289-449 (1999).

[6] C.T. CROWE, T.R. TROUTT and J.N. CHUNG - *Multiphase Flows with Droplets and Particles*. CRC Press (1998).

[7] E. DANIEL, R. SAUREL, M. LARINI and J.C. LORAUD - *A Comparison Between Centered and Upwind Schemes for Two-Phase Compressible Flows*. AIAA n°2346 (1993).

[8] O. DESJARDINS, R.O. FOX and P. VILLEDIEU - *A Quadrature-Based Moment Method for Dilute Fluid-Particle Flows*. Journal of Computational Physics 227, pp. 2514-2539 (2008).

[9] F. DOISNEAU, F. LAURENT-NEGRE, A. MURRONE, J. DUPAYS and M. MASSOT - *Optimal Eulerian Model for the Simulation of Dynamics and Coalescence of Alumina Particles in Solid Propellant Combustion.* 7th International Conference on Multiphase Flow (2010).

[10] G. DUFOUR and P. VILLEDIEU - *A Second Order Multi-Fluid Model for Evaporating Sprays.* M2AN, Vol. 39-5, pp. 931-963 (2005).

[11] J.K. DUKOWICZ - *A Particle-Fluid Numerical Model for Liquid Sprays.* Journal of Computational Physics, 35, pp. 229–253 (1980).

[12] P. FEVRIER - *Etude numérique des effets de concentration préférentielle et de corrélation spatiale entre vitesses de particules solides en turbulence homogène isotrope stationnaire.* Ph.D. Thesis, INP-Toulouse (2000).

[13] P. FEVRIER, O. SIMONIN and K.D. SQUIRES - *Partitioning of Particle Velocities in Gas-Solid Turbulent Flows into a Continuous Field and a Spatially Uncorrelated Random Distribution: Theoretical Formalism and Numerical Study.* J. Fluid Mech. 533, 146 (2005).

[14] N. GARCIA-ROSA, P. VILLEDIEU, J. DEWITTE and G. LAVERGNE - *A New Droplet-Wall Interaction Model.* 10th International Congress on Liquid Atomization and Spray Systems, ICLASS 2006, KYOTO, 27 August-1 September (2006).

[15] J.B. GREENBERG, I. SILVERMAN and Y. TAMBOUR - *On the Origins of Spray Sectional Conservation Equations*. Combustion and flame 93, pp. 90-96, (1993).

[16] C.W. HIRT and B.D. NICHOLS - *Volume of Fluid (VOF) Method for the Dynamics of Free Boundaries*. Journal of Computational Physics, 39 : pp. 201–225 (1981).

[17] J. HYLKEMA - *Modélisation cinétique et simulation numérique d'un brouillard dense de goutelettes. Application aux propulseurs à poudre*. Ph.D. Thesis ENSAE (1999).

[18] M. ISHII - *Thermo-Fluid Dynamic Theory of Two-phase flow.* Volume 22 of Direction des etudes et recherches d'électricité de France. Eyrolles, Paris, (1975).

[19] A.K. KAPILA, R. MENIKOFF, J.B. BDZIL, S.F. SON and D.S. STEWART - *Two-Phase Flow Modelling of DDT in Granular Materials : Reduced Equations*. Phys. Fluid, Vol. 13, pp. 3002-3024 (2001).

[20] F. LAURENT, M. MASSOT and P. VILLEDIEU - *Eulerian Multi-Fluid Modelling for the Numerical Simulation of Coalescence in Polydisperse Dense Liquid Sprays*. Journal of Computational Physics, 194 (2), pp. 504-543 (2004).

[21] N. LE LOSTEC, R.O. FOX, O. SIMONIN and P. VILLEDIEU - *Numerical Description of Dilute Particle Laden Flows by a Quadrature-Based Moment Method.* Annual Briefs 2008 of Center for Turbulence Research, Stanford, USA (2008).

[22] R.J. LEVEQUE - *The Dynamics of Pressureless Dust Clouds and Delta Waves.* J. Hyperbolic Differential Equations, Vol. 1, pp. 315-327 (2004).

[23] E. MONTREUIL, A. CHAZOTTES, D. GUFFOND, A. MURRONE, F. CAMINADE and S. CATRIS - *Enhancement of Prediction Capability in Icing Accretion and related Performance Penalties.* Part I: Three-dimensional CFD Prediction of the Ice Accretion. AIAA n°3969 (2009).

[24] A. MURRONE and H. GUILLARD - *A Five Equation Reduced Model for Compressible Two Phase Flow Problems.* Journal of Computational Physics, 202, pp. 664–698 (2005).

[25] A. NICOLE - *Simulation du cas Mascotte subcritique LOX/GH2 (10 bar)*. Onera RT n°1/11889 DEFA, September (2007).

[26] A. NICOLE - *Simulation du cas Mascotte subcritique LOX/GH2 (10 bar) en 3D.* Onera RT n°4/13989 DEFA, December (2008).

[27] A. NICOLE - *Simulation aux grandes échelles du cas Mascotte subcritique LOX/GH2 (10 bar) en 3D.* Onera RT n° 14450/06F, December (2009).

[28] P.J. O'ROURKE - *Collective Drop Effects on Vaporizing Liquid Sprays.* Ph.D. Thesis, Los Alamos National Laboratory, New Mexico (1981).

[29] C. RABE - *Etude de la coalescence dans les rampes de spray : application au système d'aspersion des Réacteurs a Eau Pressurisée*. Ph.D. Thesis, University of Paris 6 (2009)

[30] A. REFLOCH, G. CHAINERAY, B.COURBET, J.B. DARGAUD, P. GILBANK, C. LAURENT, A. MURRONE, E. QUEMERAIS, P. VILLEDIEU, L. TESSÉ, J. TROYES and F.VUILLOT - *CEDRE Software*. Aerospace Lab Journal Issue 2 (2011).

[31] E. RIBER, M. GARCIA, V. MOUREAU, H. PITSCH, O. SIMONIN and T. POINSOT - *Evaluation of Numerical Strategies for LES of Two-Phase Reacting Flows.* Proc of the Summer Program (2006), Center for Turbulence Research, NASA Ames/Stanford Univ., pp. 197–213. 67 (2006).

[32] M. RUGER, S. HOHMANN, M. SOMMERFELD and G. KOHNEN - *Euler/Lagrange Calculations of Turbulent Sprays : the Effect of Droplet Collisions and Coalescence.* Atomization Sprays 10 (1) (2000).

[33] P.G. SAFFMAN - *The Lift on a Small Sphere in a Shear Flow.* Journal of fluid Mechanics. 22, pp. 385-400 (1965).

[34]. R. SAUREL and R. ABGRALL - *A Multiphase Godunov Method for Compressible Multifluid and Multiphase Flows*. Journal of Computational Physics, 150, pp. 425-467 (1999).

[35] O. SIMONIN - *Continuum Modelling of Dispersed Turbulent Two Phase Flows. Combustion and Turbulence in Two Phase Flows,* VKI lecture series, (1996).

[36] D.B. SPALDING - *The Combustion of Liquid Fuels. In Proceedings of the 4th Symp International on Combustion,* the Comb Institute, pp. 847-864, Baltimore (1953).

[37] M. SUSSMAN, M. SMEREKA and S. OSHER - *A Level-Set Approach for Computing Solutions to Incompressible Two-Phase Flows*. Journal of Computational Physics, 114, pp. 146–159 (1994).

[38] B. VAN LEER - T*owards the Ultimate Conservative Difference Schemes V. A Second Order Sequel to Godunov's Method.* Journal of Computational Physics, 32, pp. 101-136 (1979).

[39] P. VILLEDIEU and O. SIMONIN - *Modelling of Coalescence in Turbulent Gas-Droplet Flows,* Communication in Mathematical Science, Supplemental Issue, No. 1, pp 13-33 (2004).

[40] F.A. WILLIAMS - *Spray Combustion and Atomization.* Physic of Fluid, 1, pp. 541-545 (1958).

[41] F.A. WILLIAMS - *Combustion Theory (Combustion Science and Engineering Series).* Ed F A Williams, Reading, MA, Addison-Wesley (1985).

[42] S. WIROGO and S. SRIRAMBHATLA - *An Eulerian Method to Calculate the Collection Efficiency on Two and Three Dimensional Bodies*. AIAA n°1073, (2003).

Acronyms

n.d.f (number density function)

p.d.f (probability density function)

DPS (Discrete Particle Simulation method)

SLD (Supercooled Large Droplet)

AUTHORS

Angelo Murrone is a senior scientist in the Fundamental and Applied Energetics Department at Onera. His research concerns the numerical modeling of "dispersed" and "separated" two-phase flows. He is currently in charge of the development of the Eulerian solver SPIREE in the CEDRE multi-physics Code.

Philippe Villedieu is a senior scientist in the Multiphase Flow Research Unit at Onera and associate professor at the National Institute of Applied Science (INSA) of Toulouse. He is in charge of the development of the SPARTE solver, which is the Lagrangian spray module in CEDRE